Spatial modeling of red spider mite *Oligonychus punicae* (Acari: Tetranychidae) in avocado crop

Fidel Lara-Vázquez[1], José Francisco Ramírez-Dávila[2,*], Dulce Karen Figueroa-Figueroa[1], Atenas Tapia-Rodríguez[1], and Andrés González-Huerta[1]

Abstract

In recent years, there has been a rising concern in society to produce quality food in a sustainable manner. New alternatives in pest control have been researched to help mitigate the environmental impact. In traditional agriculture, pesticides are applied uniformly, without considering spatial and temporary variables, but application rates could be adjusted according to the incidence with the assistance of distribution maps; thus, contributing to improve environmental balance and production costs. Avocado (*Persea americana* Mill.; Lauraceae) generates huge economic benefits in the localities where it is grown. Red spider mite (*Oligonychus punicae* Hirst.; Acari: Tetranychidae) is among the main pests that attack this crop. It causes damage to the epidermis of the leaves in such a way that the injured areas discolor and the edges of the leaves are deformed as a result of the removal of the cellular content from the tissues. Therefore, the objective of the present work was the determination of the spatial pattern of this pest, by means of geostatistics and spatial analysis by distance indices (SADIE). The adjusted semivariograms as well as the indices show that the red spider mite is distributed in aggregations. The generated maps showing the infested surface will permit pest management programs to direct control measures to the areas with the highest incidence, resulting in a lower level of economic damage.

Key Words: mites; geostatistics; kriging; density maps; SADIE

Resumen

En los últimos años ha aumentado la preocupación de la sociedad por producir alimentos de calidad de forma sostenible. Se han investigado nuevas alternativas en el control de plagas para ayudar a mitigar el impacto ambiental. En la agricultura tradicional, los plaguicidas se aplican de manera uniforme, sin tener en cuenta variables espaciales y temporales, pero las dosis de aplicación podrían ajustarse en función de la incidencia con la ayuda de mapas de distribución; contribuyendo así a mejorar el equilibrio medioambiental y los costes de producción. El aguacate (*Persea americana* Mill.; Lauraceae) genera enormes beneficios económicos en las localidades donde se cultiva. La araña roja (*Oligonychus punicae* Hirst.; Acari: Tetranychidae) es una de las principales plagas que atacan a este cultivo. Provoca daños en la epidermis de las hojas de tal forma que las zonas lesionadas se decoloran y los bordes de las hojas se deforman como consecuencia de la eliminación del contenido celular de los tejidos. Por ello, el objetivo del presente trabajo fue la determinación del patrón espacial de esta plaga, mediante geoestadística y análisis espacial por índices de distancia (SADIE). Los semivariogramas ajustados así como lo índice muestran que la araña roja se distribuye en agregaciones. Los mapas generados mostrando la superficie infestada permitirán a los programas de control de plagas dirigir las medidas de control a las zonas con mayor incidencia, lo que redundará en un menor nivel de daños económicos.

Palabras Clave: ácaros; geoestadística; kriging; mapas de densidad; SADIE

Avocado (*Persea americana* Mill.; Lauraceae) cultivar 'Hass' is one of the main fruit crops in Mexico due to its importance in national and international markets. Its worldwide production is estimated at 4.2 million tons. Mexico is the most important producer with an annual average production of 1.8 million tons distributed in 205 thousand ha, with a yield of 10.18 ton/ha (SIAP 2019).

Avocado crops present many pests, among them: thrips (*Frankliniella* spp.; Thysanoptera: Thripidae), mites (*Oligonychus punicae* Hirst. and *O. perseae* Tuttle; Acari: Tetranychidae), trunk and branch borer (*Copturus aguacatae* Kissinger; Coleoptera: Curculionidae), avocado leafhopper (*Idona minuenda* Ball; Hemiptera: Cicadellidae), whiteflies (*Tetraleurodes* spp.; Hemiptera: Aleyrodidae), avocado leafroller (*Amorbia cunneana* Walsingham; Lepidoptera: Tortricidae), avocado leafminer (*Gracilaria perseae* Busck; Lepidoptera: Gracillariidae), and avocado seed borers (*Conotrachelus perseae* Barber and *C. aguacatae* Barber; Coleoptera: Curculionidae) (Equihua-Martínez et al. 2016).

Among the pests, the mite *O. punicae*, also known as the red spider mite, has become important to avocado crops because it feeds on the foliage, by inserting its stylet into the plant tissue, causing reddish spots. When damage is severe, it causes the collapse of the mesophyll, which results in defoliation and reduction in production. The mite is present all year round in Mexico, but its highest incidence is in spring and autumn. This pest is distributed in North and South America, as well as in European and Asian countries (Chávez-Acosta 2020). Tradi-

tionally, to control this pest, chemical products were utilized, however they have lost their efficacy due to misuse, which has resulted in the development of resistance (Correa-Méndez et al. 2018).

There have been numerous investigations in spatial distribution modelling of insects, diseases, and mites in avocado. In relation to insects, Acosta-Guadarrama et al. (2017) carried out a study using geostatistical techniques to study spatial distribution of *Thrips* spp. (Thysanoptera) and assessment of its control by the predator *Amblyseius swirskii* Athias-Henriot (Acari: Phytoseiidae) in avocado crops. On the topic of diseases, Osorio-Almanza et al. (2017) worked with spatial distribution of the potential risk of avocado wilting caused by *Phytophtora cinnamomi* (Pythiaceae). With regards to mites, Landeros et al. (2003) studied the spatial distribution and population fluctuation of *Phyllocoptruta oleivora* (Ashmead) (Acari: Eriophyidae) in citrus crops and López- López et al. (2011) studied spatial distribution and effect of population densities of *Tetranychus urticae* Koch on feed corn yield. The use of techniques to model spatial distribution has proven to be an efficient tool to determine the spatial distribution of pests and diseases allowing pest managers to locate aggregations so that targeted management strategies can be carried out in economically important crops (Rivera-Martínez et al. 2017; Lara-Díaz et al. 2020).

Spatial analysis by distance indices (SADIE) identify the spatial model for two-dimensional data, with an associated index of aggregation and a test for deviation from randomness based on an attraction algorithm, which incorporates a biological model for the dispersion of individuals from an origin in which each individual is assigned a dynamic territory. Perry et al. (1996) indicated that for data collected at specific locations the use of distance for regularity is well suited and demonstrated how to distinguish non-randomness in the form of statistical heterogeneity from spatial non-randomness. Perry et al. (1996) developed and extended the use of the distance index for regularity (*Ia*) for establishing the spatial structure of insect populations. In addition, he introduced 2 diagnostic diagrams to aid interpretation and a new index for estimating the number of cluster foci in a population, the *Ja* index.

Monitoring *O. punicae* populations is necessary to understand how mite populations are distributed in avocado crops, which would help elaborate control strategies (Liang et al. 2020). Therefore, the objective of the present work was to determine the spatial distribution of *O. punicae* in avocado crops using geostatistical techniques.

Materials and Methods

STUDY AREA

The study was carried out in the municipalities of Tenancingo de Degollado (18.9500000 °N, 99.5833333 °W) average altitude 2,031 masl and Temascaltepec (19.0233333 °N, 100.0227778 °W) average altitude 1,740 masl, in eight 2-ha plots per municipality. All plots were subject to the same agronomic management without application of pesticides during the measurement period. In all plots the age of the trees was greater than 8 yrs and with a foliar coverage between trees close to 100%. In the study area there are 2 seasons of vegetative growth (Dec–Apr and Oct–Nov), flowering (Dec–Feb and Aug–Oct), harvesting (Nov–Feb and Aug–Oct), and root growth (Apr–Jul and Oct–Dec). Sampling was done by quadrant methodology, which consisted of dividing the plot in 50 quadrants of 20 × 20 m. Twenty-five quadrants were randomly taken per plot where 2 trees were selected, each 1 of the 50 trees per plot was marked and georeferenced using a GPSmap60 (Garmin) to obtain its coordinates, with a margin of error of 2 to 3 m.

SAMPLING OF MITES

A monthly sampling was carried out from Oct 2019 to May 2020. The number of mites per leaf was counted with a 20× magnification lens. Sixty leaves per tree were selected taking 5 leaves in each of 3 strata (lower, middle, and upper), in each cardinal point of the tree (north, east, west, and south) (González 2012; Ramírez Dávila & Figueroa Figueroa 2013; Maldonado-Zamora et al. 2017).

DATA ANALYSIS

A statistical exploration was carried out in the original data populations of *O. punicae* for each sampling. The asymmetry coefficient and the kurtosis test were used to determine the normality of the data. It was determined that all data had a normal distribution (Martínez-Martínez et al. 2021).

Geostatistical Analysis

The experimental semivariogram was estimated with data obtained from samples of *O. punicae* (Isaaks & Srivastava 1989; Pasini et al. 2020). The experimental semivariogram obtained was adjusted to a theoretical semivariogram. The theoretical models used were spherical and gaussian. Finally, nugget effect, sill, and range values were determined (Englund & Sparks 1988; Maldonado-Zamora et al. 2017; Contreras Velásquez 2020).

Validation of the theoretical model was carried out interactively, varying the values 'Co' (nugget effect), 'C + Co' (sill) and 'a' (range), until the best fit was obtained. Once these values were determined, they were validated through the determination of cross validation statistical parameters such as: mean of estimation errors (MEE), mean quadratic error (ECM) and mean dimensionless quadratic error (ECMA) (Tapia Rodríguez et al. 2020).

The level of spatial dependence was calculated to determine the degree of relationship that the corresponding data store. This value is obtained by dividing the nugget effect by the sill, and the result is expressed as a percentage, less than 25% is high spatial dependence, between 26 and 75% is moderate and over 76% is low (Cambardella et al. 1994).

Finally, once the semivariogram models were validated, density maps were produced. The spatial interpolation was performed using the ordinary kriging method, which allows the estimation of values associated to points that were not sampled. The program Surfer 9 (Surface Mapping System, Golden Software Inc., Golden, Colorado, USA) was used to prepare the density maps. The estimation of the infested surface was carried out using the density maps for each sampled date (Tapia Rodríguez et al. 2020).

Estimation of the spatial analysis by distance indices (SADIE) *Ia* and *Ja*

According to Ramírez-Dávila et al. (2012) individuals are the sampling units i = 1,.... n, remaining two-dimensionally (Xi, Yi) for each sampling unit, their count is contained in Ni; the aggregation index *Ia* is defined as *Ia* =D/Ea, where *D* (distance for regularity) is the minimum value of the distance in which the individuals could have moved from one sampling unit to another and *Ea* is the distance of the arithmetic mean for the regularity of the samples. *Pa* (probability of aggregation) represents the proportion of samples selected randomly with distance for regularity as big as, or bigger than, the observed value, *D*. With respect to *Pa* (probability of aggregation), the null hypothesis can be rejected, if *Pa* < 0.025 (in favor of an alternative hypothesis), or if *Pa* > 0.975 (in favor of the regularity alternative) given the usual 5% prob-

ability. The aggregation index *Ja,* on the other hand, is given as *Ja = Fa /C*, where *Fa* is the average clustering distance for random samples and *C* (distance for clustering) is the value of the distance that individuals must move to congregate in a unit. Random permutations of the observed counts lead to a ratio called *Qa* (clustering probability) with a very small distance to the clustering, or less than the observed value, *C.* With respect to *Qa* (clustering probability) the null hypothesis of randomness can be rejected if *Qa* < 0.025 (in favor of the aggregation alternative) or if *Qa* > 0.975 (in favor of the regularity alternative).

Therefore, the sample is aggregated if *Ia* > 1, it is random if *Ia* = 1 and it is regular if *Ia* < 1; on the other hand, if *Ja* > 1 the sample is aggregated, if *Ja* = 1 it is spatially random and if *Ja* < 1 the sample is regular. The values of *Ja* index are used to confirm the results obtained with the *Ia* index. To determine the significance with respect to the unit its respective probability is used (*Qa*) (Perry 1998). The program used was SADIE 1.2 (Perry et al. 1996).

Results

It was possible to carry out the modeling and mapping of the populations of *O. punicae* in the avocado plots with the results of the monthly sampling. It was also possible to determine the spatial behavior of this mite in the short term, establishing the percentage of infestation in each sampling per plot.

The average populations of *O. punicae* varied within plots and date of sampling; for Tenancingo municipality the lowest density was registered in Dec in plot 1 with 21.62 mites per leaf; for Temascaltepec municipality the lowest average density was registered in plot 5 in Nov with 41.02 mites per leaf. The highest densities were registered in May with 288.64 and 328.58 mites per leaf in plots 4 and 5 in the municipalities of Tenancingo and Temascaltepec, respectively (Table 1).

The spatial distribution in commercial avocado plots presented by *O. punicae* was aggregated on all the sample dates. The experimental semivariograms obtained in the plots for Tenancingo municipality best fitted the spherical (17) and gaussian (15) models; in plot 1 in Nov and May they best fitted the gaussian model, the rest of the months they best fitted the spherical model. In the municipality of Temascaltepec, experimental semivariograms best fitted the spherical (22) and gaussian (10) models; in plot 8, Oct, Apr and May the dataset best fitted the gaussian model, the rest of the months best fitted the spherical model (Table 1). For all fitted models the nugget effect was zero, so the sampling error was considered minimal and the sampling scale for each locality was appropriate.

The range indicates the maximum distance to which there is a spatial relationship between the data; the range values that were presented for plot 1 belonging to Tenancingo were located between 22.00 m in Jan and 39.10 m in Dec, in this municipality the minimum range was 12.79 m and the maximum range was 49.70 m corresponding to plot 2 in Oct and plot 3 in Dec, respectively. For Temascaltepec municipality in plot 6 the range values fluctuated between 25.50 m and 43.50 m in Nov and Feb, respectively, for total sampling in the municipality, the minimum range was 13.87 m in plot 8 in Nov, and the maximum range was 45.00 m in plot 5 in Mar (Table 1).

The fitted models in each sample showed a high level of spatial dependence. The models that resulted from the spatial distribution of *O. punicae* were validated with the statistical parameters locating them within allowable range.

Density mapping was carried out using the geostatistical method known as ordinary kriging once the corresponding semivariograms were validated. In these maps it was observed that *O. punicae* was distributed in specific aggregations in different plot areas. Of the sam-

plings carried out in the different plots, examples are described below by municipality.

In the case of plot 1 of Tenancingo municipality, the surface density for Oct, Nov, and Dec show that aggregations were distributed in the central area of the plot with a tendency towards the left side, in Jan, Feb, and Mar, aggregations were randomly distributed on the edges of the plot, yet in Apr the infestation sites were located on the right side with a tendency towards the center; finally, in May there was only 1 significant aggregation on the left side. It is noteworthy that in the last 2 mo (Apr and May) the highest number of *O. punicae* is present due to the lack of rain in the study area favoring population growth (Fig. 1).

In plot 5 of Temascaltepec municipality in Oct and Nov the infestation sites were in the central area and on the left and right edges of the plot; with a downward trend on the left and towards the top on the right side, this behavior is persistent with minimal mobility. In Dec and Jan, the infestation sites were concentrated in the central part with a tendency towards the left side at the bottom and towards the right side at the top; yet in Feb, Mar, and Apr aggregations began to regroup. Infestation sites in the central part of the plot with a trend towards the bottom. Over the next 2 mo the aggregations were distributed almost uniformly in the plot, although there were some spots where a few aggregations were present. Lastly, in May, aggregations were located in the central part of the plot (Fig. 2).

In Tenancingo municipality plot 2 presented the highest infestation in Apr with 98%, the plot with the lowest infestation was plot 4 in Nov with 83%. In Temascaltepec municipality the highest infestation percentage was in plot 8 in Mar with 97% and the lowest percentage was in Jan with 78%, as can be observed in Table 1.

In the spacial analysis by distance indices (SADIE) the highest *Ia* observed in Tenancingo municipality was registered in plot 3 in May at 1.70. the lowest was registered in plot 2 in Nov at 1.28. For comparison, the highest *Ja* value was registered in plot 4 in Apr at 1.24 and the lowest at 1.05 in plot 1 in Oct.

In Temascaltepec municipality the highest *Ia* was registered in plot 8 in Nov at 1.72 and the lowest in plot 5 in May at 1.30; similarly, the highest *Ja* value was registered on plot 5 in Apr at 1.24 and the lowest in Jan in the same plot at 1.06 (Table 2). Each *Ia* and *Ja* index was significantly higher than 1, which indicates spatial distribution of *O. punicae* populations presented aggregative patterns (*Ia* index) at various clustering aggregates (*Ja* index).

Discussion

The spatial pattern reflects the characteristic ecological property of a species therefore it is important to identify the space time dynamics of a pest to have a better understanding of spatial patterns of populations (Zhang et al. 2020).

From the ecological point of view living beings are organized in groups. These groups are made up of individuals of the same species in a given area. There is exchange of genetic information among these individuals. *Oligonychus punicae* can be found year-round in Mexico, with the highest incidence in dry and hot months of the year, regarding the sampled municipalities, such conditions are present in Apr and May. The months when the number of *O. punicae* is the lowest were Oct, Nov, and Dec, because in these months' temperatures are low; this was also observed by Márquez-Santos et al. (2020).

In the current study, the determination of the aggregated pattern in the spatial distribution model was completed using geostatistical methods. Compared with the estimation of the spatial distribution carried out with classical statistics, geostatistical methods provide a more direct measure of spatial dependence, because they consider the bidi-

Table 1. Parameters of the theoretical models fitted to the semivariograms of *Oligonychus punicae*, in the Tenancingo municipality (plots 1, 2, 3, and 4) and Temascaltepec municipality (plots 5, 6, 7, and 8).

P.	Date	Model	Mean Density	Min.	Max.	Nugget	Hill	Range	Nugget/Hill	Spatial dependence level	%
1	Oct 2016	Spherical	32.90	1	69	0	302.46	25.70	0	High	92
	Nov 2016	Gaussian	24.72	0	62	0	270.00	26.64	0	High	90
	Dec 2016	Spherical	21.62	0	55	0	228.15	39.10	0	High	88
	Jan 2017	Spherical	24.14	4	59	0	176.00	22.00	0	High	91
	Feb 2017	Spherical	52.58	27	94	0	285.80	32.56	0	High	86
	Mar 2017	Spherical	64.52	38	113	0	324.17	29.60	0	High	84
	Apr 2017	Spherical	98.18	47	180	0	662.20	32.56	0	High	85
	May 2017	Gaussian	283.76	148	528	0	2,571.40	22.95	0	High	95
2	Oct 2016	Spherical	31.38	1	65	0	319.43	12.79	0	High	89
	Nov 2016	Spherical	31.32	0	68	0	392.59	31.91	0	High	91
	Dec 2016	Gaussian	38.88	4	82	0	497.28	15.59	0	High	94
	Jan 2017	Spherical	39.68	4	83	0	622.50	29.40	0	High	90
	Feb 2017	Gaussian	49.70	5	104	0	960.00	31.17	0	High	92
	Mar 2017	Gaussian	79.44	15	133	0	1,344.76	24.00	0	High	97
	Apr 2017	Gaussian	132.70	63	193	0	845.32	31.73	0	High	98
	May 2017	Spherical	287.00	132	490	0	2,630.61	26.60	0	High	95
3	Oct 2016	Gaussian	28.94	1	59	0	273.98	20.61	0	High	88
	Nov 2016	Gaussian	29.04	2	60	0	285.60	28.88	0	High	87
	Dec 2016	Spherical	33.32	5	62	0	289.57	49.70	0	High	90
	Jan 2017	Spherical	34.00	4	68	0	348.30	34.00	0	High	91
	Feb 2017	Gaussian	41.66	7	79	0	508.40	26.60	0	High	86
	Mar 2017	Spherical	72.52	20	117	0	653.73	33.44	0	High	93
	Apr 2017	Gaussian	116.76	55	190	0	1,130.59	26.67	0	High	90
	May 2017	Spherical	282.30	130	467	0	3,333.33	28.94	0	High	96
4	Oct 2016	Spherical	32.12	1	62	0	270.00	17.88	0	High	87
	Nov 2016	Spherical	33.02	2	75	0	370.92	35.45	0	High	83
	Dec 2016	Gaussian	36.00	1	73	0	379.16	28.79	0	High	87
	Jan 2017	Gaussian	40.40	3	83	0	397.34	25.85	0	High	93
	Feb 2017	Gaussian	56.58	16	104	0	489.75	24.85	0	High	95
	Mar 2017	Spherical	65.50	21	113	0	570.00	35.25	0	High	94
	Apr 2017	Gaussian	104.68	52	172	0	861.26	30.75	0	High	89
	May 2017	Gaussian	288.64	175	520	0	2,283.31	28.69	0	High	91
5	Oct 2016	Gaussian	43.94	13	63	0	256.00	26.62	0	High	92
	Nov 2016	Spherical	41.02	3	74	0	247.77	30.75	0	High	91
	Dec 2016	Spherical	44.56	12	82	0	230.33	30.00	0	High	88
	Jan 2017	Spherical	46.64	14	82	0	206.30	39.75	0	High	89
	Feb 2017	Gaussian	57.72	18	86	0	329.89	28.50	0	High	95
	Mar 2017	Spherical	67.66	17	97	0	405.00	45.00	0	High	96
	Apr 2017	Spherical	143.14	79	179	0	619.47	27.99	0	High	89
	May 2017	Gaussian	328.58	185	480	0	2,628.37	24.08	0	High	94
6	Oct 2016	Spherical	48.98	17	82	0	344.64	27.59	0	High	84
	Nov 2016	Gaussian	45.14	9	87	0	367.50	25.50	0	High	87
	Dec 2016	Spherical	47.06	14	81	0	286.99	36.49	0	High	85
	Jan 2017	Spherical	54.04	17	83	0	272.89	33.00	0	High	86
	Feb 2017	Spherical	59.54	16	86	0	264.66	43.50	0	High	91
	Mar 2017	Spherical	76.14	37	97	0	200.82	40.50	0	High	93
	Apr 2017	Spherical	104.98	55	230	0	768.48	37.50	0	High	90
	May 2017	Spherical	292.28	80	539	0	3,530.96	37.48	0	High	95
7	Oct 2016	Spherical	53.64	17	85	0	410.34	20.68	0	High	81
	Nov 2016	Gaussian	53.42	13	84	0	369.61	14.60	0	High	93
	Dec 2016	Gaussian	58.48	22	93	0	436.71	17.52	0	High	90
	Jan 2017	Spherical	61.80	23	97	0	429.49	13.90	0	High	78
	Feb 2017	Gaussian	72.54	32	108	0	424.91	15.25	0	High	93
	Mar 2017	Spherical	84.06	48	118	0	386.07	21.17	0	High	90
	Apr 2017	Spherical	106.84	60	245	0	895.93	31.20	0	High	92
	May 2017	Spherical	292.86	140	461	0	3,786.93	23.60	0	High	91

P. = plot, Mín. = minimum number of mites per tree, Max. = maximum number of mites per tree, % = infested surface.

Table 1. (Continued) Parameters of the theoretical models fitted to the semivariograms of *Oligonychus punicae*, in the Tenancingo municipality (plots 1, 2, 3, and 4) and Temascaltepec municipality (plots 5, 6, 7, and 8).

P.	Date	Model	Mean Density	Min.	Max.	Nugget	Hill	Range	Nugget/Hill	Spatial dependence level	%
8	Oct 2016	Gaussian	50.19	7	74	0	453.70	14.56	0	High	88
	Nov 2016	Spherical	58.72	13	95	0	480.76	13.87	0	High	90
	Dec 2016	Spherical	60.94	18	100	0	430.08	18.25	0	High	92
	Jan 2017	Spherical	70.00	24	104	0	469.80	16.79	0	High	91
	Feb 2017	Spherical	82.64	25	110	0	375.07	17.76	0	High	95
	Mar 2017	Spherical	92.76	37	120	0	330.30	24.09	0	High	97
	Apr 2017	Gaussian	127.20	76	225	0	959.07	23.90	0	High	86
	May 2017	Gaussian	294.56	145	520	0	3,383.73	19.23	0	High	92

P. = plot, Mín. = minimum number of mites per tree, Max. = maximum number of mites per tree, % = infested surface.

mensional nature of the organisms through their exact spatial location and it is independent of the relationship between mean and variance (Ramírez Dávila et al. 2013; Rivera-Martínez et al. 2017).

With geostatistics it is possible to describe the spatial continuity of any natural phenomenon. Furthermore, it is possible to know the way any continuous variable in space varies (spatial pattern) in one or several selected scales, with a level of detail that allows the quantification of the spatial variance of the variable in different directions of space. Geostatistics uses functions to model this spatial variation, these functions are used to interpolate in space the variable value in non-sampled sites in addition, it makes it possible to draw up useful maps of the spatial distribution of an organism (Tapia Rodríguez et al. 2020).

Spatial behavior under conditions of infestation of *O. punicae* in avocado presented an aggregated pattern. This result suggests that handling this mite can be achieved by directing its control to specific points or infestation sites where aggregations are located, avoiding the widespread application of chemical products in avocado commercial plots, helping to minimize environmental deterioration and saving inputs by producers. This result agreed with Ramírez Dávila and Pocayo Camargo (2009), who worked with *Jacobiasca lubica* Bergenin & Zanon (Homoptera: Cicadellidae) (known as green mosquitoes) on vine, they indicated that knowing the infested surface on the maps makes it possible to establish the expenses and economic savings regarding the application of insecticides, carrying out control measures directed to infested areas.

The fitted models have a 98% reliability, consequently, it is valid to deduce that more than 90% of the total variance is due to the spatial dependence on the sampling scale used. In other words, over 90% of the variation in the distribution of the population of this mite was explained with the spatial structure established in the semivariograms (Liebhold & Sharoy 1998; Rivera-Martínez et al. 2017). Esquivel Higuera and Jasso Gárcia (2014), in their work on the distribution of armyworm *Mythimna unipuncta* Haworth (Lepidoptera: Noctuidae) in corn, found nugget effect values close to zero, which points out that in its totality the variation of the pest distribution was explained by the spatial structure in the semivariograms (Ramírez Dávila et al. 2013; Rivera-Martínez et al. 2017)

Datasets that best fitted the gaussian model showed the spatial behavior expressed continuously within the avocado plots, indicating a continuous progress of infestation of *O. punicae* in neighboring trees. This also was observed by Quiñones-Valdez et al. (2020), in their research on spatial modeling of thrips, in husk tomato, where semivariograms fitted the gaussian model in most of the sampled dates. Thrips eggs are present continuously within the plots, inferring the existence of several factors that influenced the spread of females to oviposit faster. Maldonado-Zamora et al. (2017) in their research on spatial sta-

bility and temporary distribution of thrips in avocado, point out that the samples that fitted the gaussian model, reflect the aggregations are presented continuously within the plot.

Datasets that best fitted the spherical model indicate that *O. punicae* aggregation occurs in greater quantity in certain areas of the plot with respect to the rest of the points considered in the sampling. The aggregation clusters are random within the infestation site of the plot, these aggregation clusters show a rapid growth near the origin but as they move away they decrease as a result of the dissemination of the mite through the wind, which results in infestation in specific sites.

Ramírez-Dávila and Esquivel Higuera (2012), in their work on armyworm (*M. unipucta*) in corn, point out that the spatial distribution of the dataset that best fitted the spherical model, show sites where armyworm manifests itself most. Variation in armyworm presence is likely due to temperature and crop phenology (Ni et al. 2003). Acosta-Guadarrama et al. (2017), in their research on spatial distribution of thrips and its control through the predator *A. swirskii* in avocado, pointed out that the spherical model was the best fit for the dataset, indicating that aggregations of insects occur in certain areas of the plot with respect to the other points. The models that best fitted the datasets (spherical and gaussian), are indicative that *O. punicae* does not have an established spatial behavior, because climatic factors such as: temperature, humidity, exposure to sun, among others influence the spatial distribution of the mite; therefore the present study is of great interest because it details the patterns of movement and permanence at specific points where preventive management programs can be performed at the aggregations and thereby maintain low infestation levels with economic savings.

The spatial dependence of *O. punicae* is high because the result of the division of the value of the nugget effect by the value of the hill was less than 25% for all semivariograms. The values of the nugget effect indicate that there is a high spatial dependency, which suggests that the populations of *O. punicae* depend on each other and their aggregation level is high (Rossi et al. 1992).

The aggregations of the *O. punicae* populations can be seen in the density maps obtained with the kriging technique. The maps allow us to visualize mite-free areas and areas with presence of mites. These maps let us deduce that *O. punicae* does not invade 100% of sampled plots. This also was appreciated by Ramírez Dávila and Figueroa Figueroa (2013), who modeled the spatial distribution of the egg, nymph, and adult stages of *Bactericera cockerelli* Sulc. (Hemiptera: Triozidae) in potato. Ramírez Dávila and Figueroa Figueroa (2013) used geostatistical tools to visualize its spatial distribution through maps by means of kriging with which it was observed that the insect does not invade 100% of the surface of the plot, allowing the identification of infested and infestation free areas. On the other hand, Rivera-Martínez
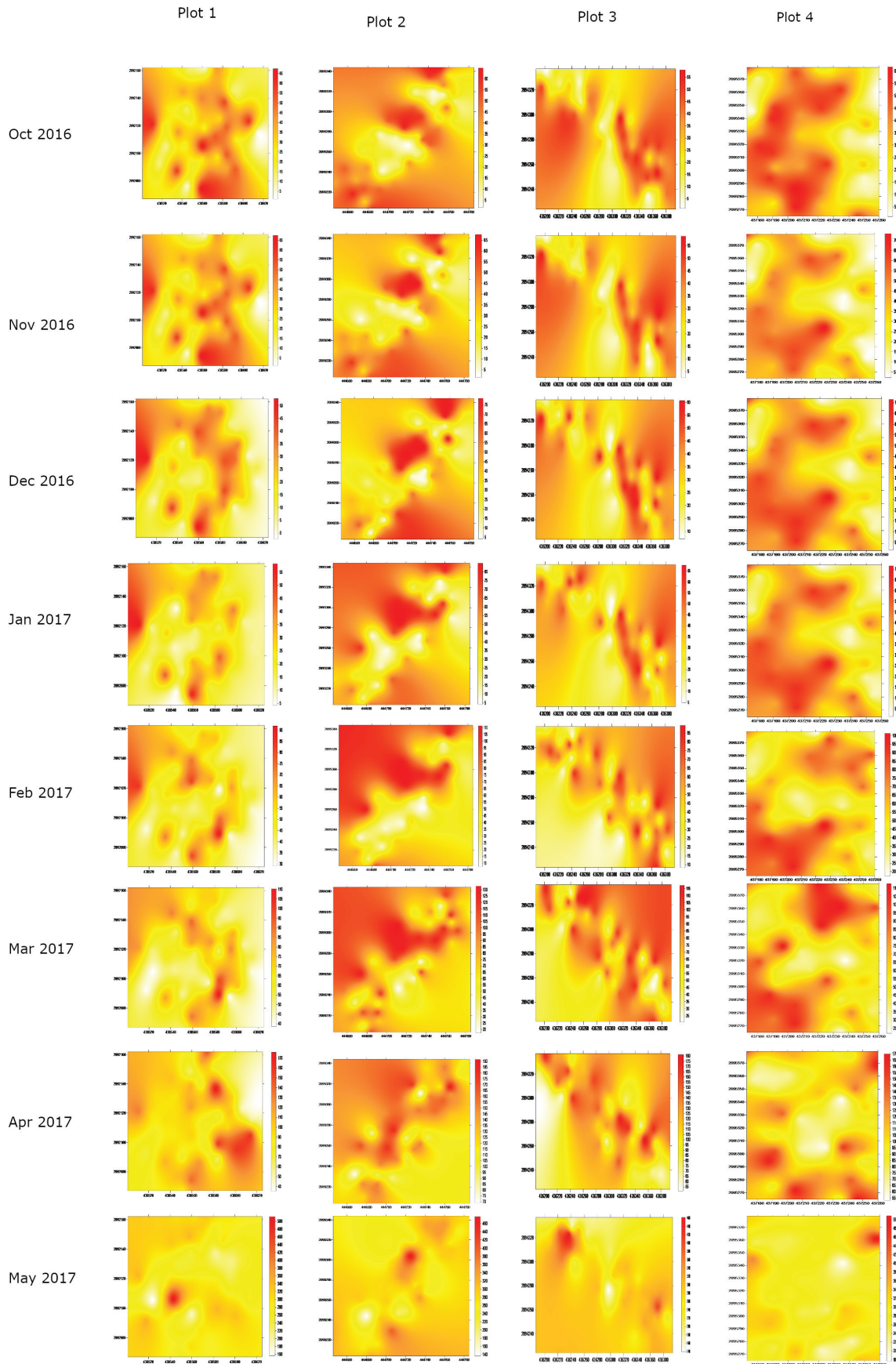
Fig. 1. Density maps of *Oligonychus punicae* Hirst, in avocado crop, by sampling month in plots of Tenancingo municipality (Mexico). Red to orange to yellow to white indicates a gradual transition from high density of *O. punicae* to an absence of the species.
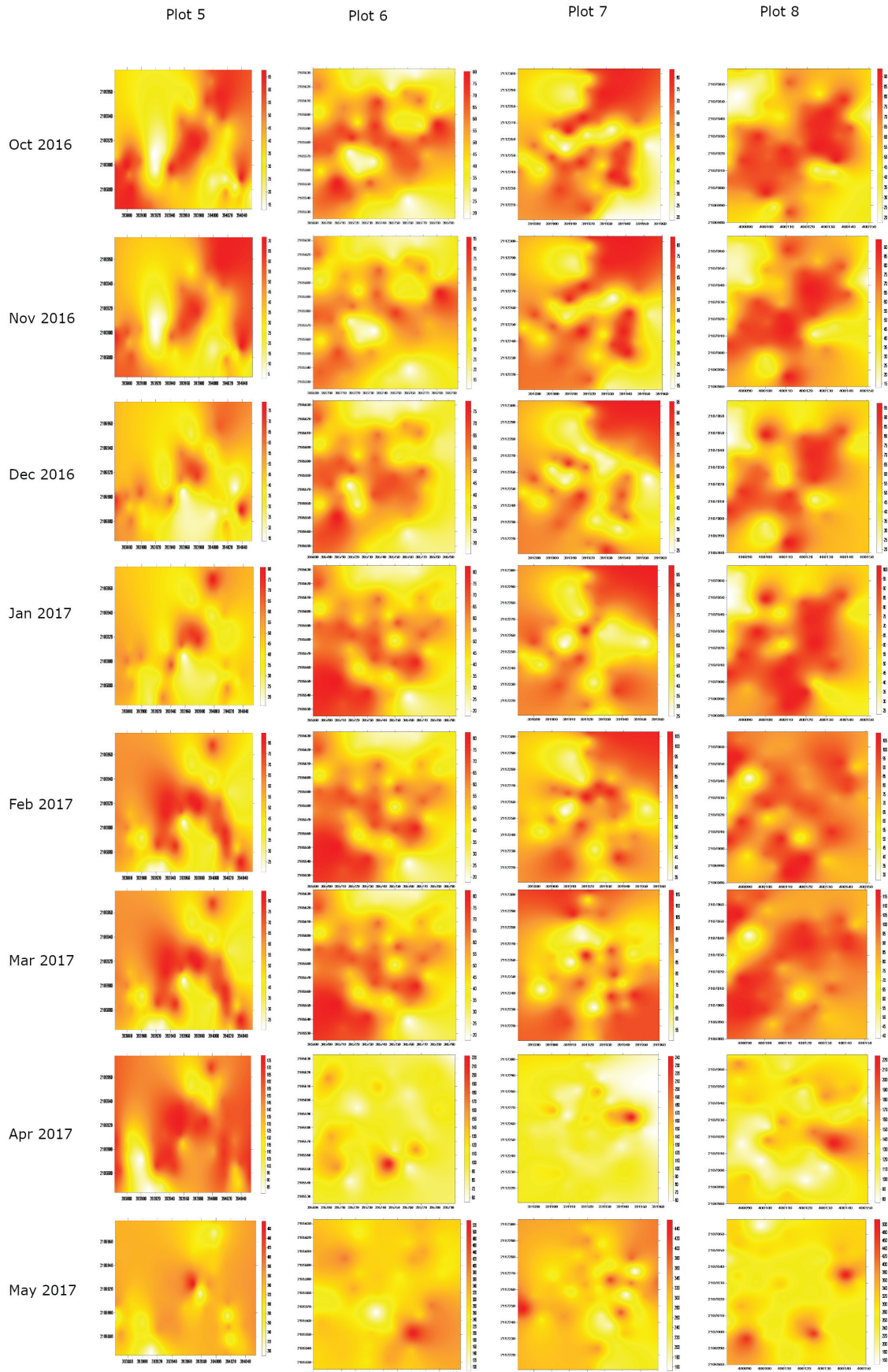
Fig. 2. Density maps of *Oligonychus punicae* Hirst, in avocado crop, by sampling month in plots of Temascaltepec municipality (Mexico). Red to orange to yellow to white indicates a gradual transition from high density of *O. punicae* to an absence of the species.

Table 2. Spacial analysis by distance indices (SADIE) in the red spider mite (*Oligonychus punicae* Hirst) population in Tenancingo (plots 1, 2, 3, and 4) and Temascaltepec (plots 5, 6, 7, and 8) municipalities. Values of the *Ia* and *Ja* indices and their respective *Pa* and *Qa* probabilities are listed.

Plot	Date	Ia	Pa	Ja	Qa
1	Oct 2016	1.34	0.005s	1.05	0.133ns
	Nov 2016	1.47	0.010s	1.10	0.178ns
	Dec 2016	1.65	0.014s	1.19	0.165ns
	Jan 2017	1.50	0.007s	1.06	0.209ns
	Feb 2017	1.36	0.006s	1.14	0.226ns
	Mar 2017	1.51	0.012s	1.15	0.249ns
	Apr 2017	1.29	0.011s	1.23	0.131ns
	May 2017	1.42	0.010s	1.20	0.262ns
2	Oct 2016	1.30	0.005s	1.10	0.275ns
	Nov 2016	1.28	0.014s	1.11	0.135ns
	Dec 2016	1.69	0.017s	1.09	0.280ns
	Jan 2017	1.36	0.009s	1.18	0.169ns
	Feb 2017	1.59	0.014s	1.17	0.238ns
	Mar 2017	1.33	0.011s	1.20	0.203ns
	Apr 2017	1.40	0.013s	1.08	0.153ns
	May 2017	1.29	0.010s	1.16	0.266ns
3	Oct 2016	1.56	0.016s	1.15	0.222ns
	Nov 2016	1.63	0.007s	1.23	0.241ns
	Dec 2016	1.48	0.015s	1.12	0.138ns
	Jan 2017	1.32	0.011s	1.11	0.271ns
	Feb 2017	1.49	0.018s	1.13	0.284ns
	Mar 2017	1.67	0.008s	1.10	0.257ns
	Apr 2017	1.38	0.013s	1.09	0.156ns
	May 2017	1.70	0.015s	1.20	0.246ns
4	Oct 2016	1.30	0.011s	1.21	0.142ns
	Nov 2016	1.55	0.005s	1.14	0.218ns
	Dec 2016	1.43	0.019s	1.13	0.204ns
	Jan 2017	1.64	0.008s	1.22	0.233ns
	Feb 2017	1.52	0.010s	1.19	0.188ns
	Mar 2017	1.41	0.013s	1.16	0.213ns
	Apr 2017	1.59	0.009s	1.24	0.147ns
	May 2017	1.60	0.012s	1.18	0.159ns
5	Oct 2016	1.32	0.011s	1.09	0.158ns
	Nov 2016	1.43	0.18s	1.13	0.134ns
	Dec 2016	1.62	0.010s	1.17	0.175ns
	Jan 2017	1.53	0.013s	1.06	0.167ns
	Feb 2017	1.49	0.014s	1.12	0.142ns
	Mar 2017	1.66	0.012s	1.08	0.208ns
	Apr 2017	1.57	0.007s	1.24	0.149ns
	May 2017	1.30	0.013s	1.19	0.229ns
6	Oct 2016	1.44	0.017s	1.15	0.289ns
	Nov 2016	1.69	0.015s	1.11	0.191ns
	Dec 2016	1.47	0.007s	1.22	0.242ns
	Jan 2017	1.45	0.012s	1.20	0.139ns
	Feb 2017	1.64	0.018s	1.16	0.251ns
	Mar 2017	1.34	0.011s	1.08	0.235ns
	Apr 2017	1.71	0.010s	1.14	0.132ns
	May 2017	1.50	0.015s	1.18	0.263ns
7	Oct 2016	1.65	0.010s	1.12	0.153ns
	Nov 2016	1.39	0.014s	1.11	0.180ns
	Dec 2016	1.51	0.016s	1.14	0.144ns
	Jan 2017	1.54	0.008s	1.09	0.196ns
	Feb 2017	1.46	0.008s	1.07	0.164ns
	Mar 2017	1.70	0.013s	1.23	0.214ns
	Apr 2017	1.65	0.011s	1.16	0.135ns
	May 2017	1.48	0.010s	1.20	0.237ns

ns: not significant at 5%, s: significant at 5%.

Table 2. (Continued) Spacial analysis by distance indices (SADIE) in the red spider mite (*Oligonychus punicae* Hirst) population in Tenancingo (plots 1, 2, 3, and 4) and Temascaltepec (plots 5, 6, 7, and 8) municipalities. Values of the *Ia* and *Ja* indices and their respective *Pa* and *Qa* probabilities are listed.

Plot	Date	Ia	Pa	Ja	Qa
8	Oct 2016	1.68	0.017s	1.18	0.172ns
	Nov 2016	1.72	0.019s	1.10	0.156ns
	Dec 2016	1.59	0.014s	1.13	0.257ns
	Jan 2017	1.41	0.009s	1.21	0.130ns
	Feb 2017	1.61	0.013s	1.11	0.249ns
	Mar 2017	1.37	0.006s	1.10	0.226ns
	Apr 2017	1.52	0.009s	1.15	0.143ns
	May 2017	1.40	0.016s	1.19	0.182ns

ns: not significant at 5%, s: significant at 5%.

et al. (2017) indicate that the maps generated by sampling for the spatial modelling of thrips in avocado crop, allowed them to identify areas of infestation, finding that thrips population were distributed in 100% of the plot. Similar results were found by Paz and Arrieche (2017), who investigated geospatial distribution and population density of *Thrips tabaci* Lindeman (Thysanoptera: Thripidae) in onion production using geostatistics. Paz and Arrieche (2017) found that the insect was present throughout the study plot, although at non-significant levels (population less than 10 individuals per plant) where no insecticide application is required because of the very low population levels, concluding that there are areas where control should be applied in a targeted way based on the population density sampled.

With regards to the values obtained from the SADIE indices, the *Ia* index was significantly greater than 1 in the different samplings; these results suggest that *O. punicae* is distributed in aggregative patterns. Regarding the *Ja* index, similar results were obtained, it was significantly greater than 1, which indicates that *O. punicae* spatial distribution is located on the entire surface concentrated in aggregations. This is reflected in the obtained maps corroborating the points made by the indices *Ia* and *Ja* (Figs. 2 and 3). Temporal stability of spatial distribution with SADIE has been reported in other papers such as Thomas et al. (2001), in which they worked with aggregation and temporal stability of the distribution of carabid beetles in field habitats; Esquivel Higuera and Jasso Gárcia (2014), with the spatial distribution and mapping of armyworm *M. unipuncta* in corn, and Maldonado-Zamora et al. (2017) in the distribution of thrips in avocado crop.

In a future study, the data collected regarding the stratus (lower, middle, and upper) will be analysed to determine whether the stratus factor presents differences thus becoming another factor to consider increasing efficiency in the management of *O. punicae* populations.

The present results show that it is possible to direct control measurements towards specific zones of mite infestation, reducing the intensity of the environmental damage generated by the exclusive and unnecessary use of chemical products to control this phytosanitary problem in avocado. It is important to point out that because of the maps elaborated through kriging, it also is possible to use biological control of this mite by means of natural predators such as *Phytoseiulus persimilis* Athias-Henriot, *Amblyseius californicus* McGregor, and *Amblyseius swirskii.* Athias-Henriot (all Acari: Phytoseiidae). The maps could greatly enhance the efficiency of these control agents because they could be released in specific areas in the known presence of the pest.

In conclusion, the spatial distribution of *O. punicae* in avocado was determined with theoretical semivariograms. The semivariograms showed that the spatial behavior of the mite was in clusters within the plots. This finding was confirmed by SADIE indices. These indices showed that *O. punicae* populations present a special clus-

tered pattern distributed in several aggregation points. All these findings can be visualized on the density maps generated through kriging. These maps can be used by growers, field technicians and government officials to generate timely, relevant, efficient, and precise management programs for *O. punicae* in avocado, because they are a useful tool to direct prevention and control measurements towards specific infested zones, to reduce and maintain populations of *O punicae* under densities causing serious economic damage thus, optimizing economical resources and reducing environmental impact due to the use of agrochemicals.

Acknowledgments

References Cited

Acosta-Guadarrama AD, Ramírez-Dávila JF, Rivera-Martínez R, Figueroa-Figueroa DK, Lara-Diaz AV; Maldonado-Zamora FI, Tapia-Rodríguez A. 2017. Distribución espacial de *Trips* spp. (Thysanoptera) y evaluación de su control mediante el depredador *Amblyseius swirskii* en el cultivo de aguacate en México. Southwestern Entomologist 42: 435–446.

Cambardella CA, Moorman TB, Novak JM, Parkin TB, Karlen DL, Turco RF, Konopka AE. 1994. Field-scale variability of soil properties in central Iowa soils. Soil Science Society of America Journal 58: 1501–1511.

Chávez Acosta R. 2020. Fluctuación poblacional de *Oligonychus punicae* Hirts (Acari: Tetranychidae), y predatores en *Persea americana* Mill. "palto", provincia de Virú, La Libertad, 2016. Tesis de licenciatura. Universidad Privada Anterior Orrego, Trujillo, Perú.

Contreras Velásquez RE. 2020. Agricultura de precisión en el manejo agronómico del cultivo de maíz. Tesis de licenciatura. Universidad Técnica de Babahoyo, Babahoyo, Los Rios, Ecuador.

Correa-Méndez A, Osorio-Osorio R, Hernández-Hernández LU, Cruz-Lázaro EDL, Márquez-Quiroz C, Salinas-Hernández RM. 2018. Control químico del ácaro rojo de las palmas *Raoiella indica* Hirst (Acari: Tenuipalpidae). Ecosistemas y Recursos Agropecuarios 5: 319–326.

Englund EJ, Sparks, AR. 1988. GEO-EAS (Geostatistical environmental assessment software) user's guide (No. PB-89-151252/XAB; EPA-600/4-88/033A). Battelle Columbus Labs., Washington, DC, USA.

Equihua-Martínez A, Estrada-Venegas EG, Chaires-Grijalva MP, Acuña-Soto JA. 2016. Comportamiento de *Araptus schwartzi* Blackman (Coleoptera: Curculionidae: Scolytinae) en semillas de aguacate (Hass) en diferentes estados de madurez. Folia Entomológica Mexicana (Nueva Serie) 2: 33–38.

Esquivel Higuera V, Jasso García Y. 2014. Distribución espacial y mapeo de gusano soldado en seis localidades del Estado de México, en el año 2011. Revista Mexicana de Ciencias Agrícolas 5: 923–935.

González E. 2012. Estudio geoestadístico de la distribución espacial de adultos de araña roja (*Oligonychus punicae* Hirst) y su daño sobre el cultivo de aguacate (*Persea americana* Mill.) en la zona oriente del Estado de Michoacán, México. Tesis de licenciatura. Facultad de Ciencias Agrícolas, Universidad Autónoma del Estado de México, México.

Isaaks EH, Srivastava RM. 1989. An Introduction to Applied Geostatistics. 1st edition. Oxford University Press, New York, USA.

Landeros J, Balderas J, Badii MH, Sánchez VM, Guerrero E, Flores AE. 2003. Distribución espacial y fluctuación poblacional de *Phyllocoptruta oleivora* (Ashmead) (Acari: Eriophyidae) en cítricos de Güemez, Tamaulipas. Acta Zoologica Mexicana 89: 129–138.

Lara-Díaz AV, Ramírez-Dávila JF, Maldonado-Zamora FI, Rivera-Martínez R, Acosta-Guadarrama AD, Lara-Vázquez F. 2020. Modelización espacial de las poblaciones de *Oligonychus perseae* (Tuttle, Baker y Abatiello, 1976) en el Estado de México. Revista Fitotecnia Mexicana 43: 411–419.

Liebhold AM, Sharov AA. 1998. Testing for correlation in the presence of spatial autocorrelation in insect count data pp 111–117. *In* Baumgartner J, Brandmayr P, Manly BFJ (eds.) Population and Community Ecology for Insect Management and Conservation, Balkema, Rotterdam, Netherlands.

López-López OV, Cerna-Chavez E, Flores-Canales R, Gevara-Acevedo LP, Badii MH, Landeros-Flores J. 2011. Distribución espacial y efecto de densidades de población de *Tetranychus urticae* Koch en el rendimiento de maíz Forrajero. Revista Agraria Nueva Época- Año VIII 8: 18–23.

Maldonado-Zamora FI, Ramírez-Dávila JF, Lara-Diaz AV, Rivera-Martínez R, Acosta-Guadarrama AD, Figueroa-Figueroa DK, Rubí-Arriaga M, Tapia-Rodríguez A. 2017. Estabilidad espacial y temporal de la distribución de trips en el cultivo de aguacate en el estado de México. Southwestern Entomologist 42: 447–462.

Márquez-Santos M, Hernández-Lauzardo AN, Castrejón-Gómez VR. 2020. States of phenological development of avocado (*Persea americana* Mill.) based on the BBCH scale extended and its relationship to the incidence of anthracnose in field conditions Scientia Horticulturae 271: 109379. DOI: 10.1016/j.scienta.2020.109379

Martínez-Martínez N, Ramírez-Dávila JF, Lara-Vázquez F, Figueroa-Figueroa DK. 2021. Distribución espacial de muérdago enano en la Reserva de la Biosfera Mariposa Monarca. Colombia Forestal 24: 65–81.

Ni S, Lockwood J, Wei Y, Jiang J, Zha Y, Zhang H. 2003. Spatial clustering of rangeland grasshoppers (Orthoptera: Acrididae) in the Qinghai Lake region of northwestern China. Agriculture, Ecosystems & Environment 95: 61–68.

Osorio-Almanza L, Burbano-Figueroa O, Arcilla C AM, Vázquez B AM, Carrascal-Pérez F, Romero F J. 2017. Distribución espacial del riesgo potencial de marchitamiento del aguacate causado por *Phytophthora cinnamomi* en la subregión de Montes de María, Colombia. Revista Colombiana de Ciencias Hortícolas 11: 273–285.

Pasini MPB, Engel E, Lúcio AD, Bortolotto RP. 2020. Semivariogram models for rice stem bug population densities estimated by ordinary kriging. Acta Scientiarum, Agronomy 43: e48310. DOI: 10.4025/actasciagron.v43i1.48310

Paz R, Arrieche N. 2017. Distribución espacial de *Thrips tabaci* (Lindeman) 1888 (Thysanoptera: Thripidae) en Quíbor, Estado Lara, Venezuela. Bioagro 29: 123–128.

Perry JN, Bell ED, Smith RH, Woiwod IP. 1996. SADIE: software to measure and model spatial patterns. Modelling in Applied Biology. Aspects of Applied Biology 46: 95–102.

Perry JN. 1998. Measures of spatial pattern for counts. Ecology 79: 1008–1017.

Quiñones-Valdez R, Sánchez-Pale JR, Castañeda-Vildozola Á, Franco-Mora O, Johansen-Naime R, Mejorada-Gómez E. 2020. Comportamiento espacial y temporal de *Thrips simplex* Morison (Thysanoptera: Thripidae) en la región norte del Estado de México. Acta Zoológica Mexicana 36: 1–15.

Ramírez-Dávila JF, Esquivel Higuera V. 2012. Modelación espacial de gusano soldado (*Mythimna unipuncta*) en el cultivar del maíz, en tres municipios del Estado de México en el 2008. Boletín del Museo de Entomología de la Universidad del Valle 13: 1–15.

Ramírez Dávila JF, Porcayo Camargo E. 2009. Comportamiento espacial de las larvas del mosquito verde *Jacobiasca lybica*, en un viñedo de secano en Andalucía, España. Ciencia Ergo Sum 16: 164–170.

Ramírez Dávila JF, Figueroa Figueroa DK. 2013. Modelización y mapeo de la distribución espacial de *Bactericera cockerelli* Sulc. (Hemiptera:Triozidae) en papa en el estado de México. Centro Agrícola 40: 57–70.

Ramírez-Dávila JF, Sánchez-Pale JR, Porcayo-Camargo E, de León C. 2012. Determination of spatiotemporal stability of corn head smut (*Sporisorium reilianum*) by SADIE. Ciencia e Investigación Agraria: Revista Latinoamericana de Ciencias de la Agricultura 39: 459–471.

Ramírez Dávila JF, Solares Alonso VM, Figueroa Figueroa DK, Sánchez Pale JR. 2013. Comportamiento especial de *Trips* (Insecta: Thysanoptera), en plantaciones comerciales de aguacate (*Persea americana* Mill.) en Zitácuaro, Michoacán, México. Acta Zoológica Mexicana (Nueva Serie) 29: 545–562.

Rivera-Martínez R, Ramírez-Dávila JF, Rubí-Arriaga M, Domínguez-López A, Acosta-Guadarrama AD, Figueroa-Figueroa DK. 2017. Modelizaciòn espacial de *trips* (Insecta: Thysanoptera) en el cultivo de aguacate (*Persea americana* Mill.). Revista Colombiana de Entomología 43: 131–140.

Rossi RE, Mulla DJ, Journel AG, Franz EH. 1992. Geostatistical tools for modeling and interpreting ecological spatial dependence. Ecological Monographs 62: 277–314.

SIAP (Servicio de Información Agroalimentaria y Pesquera). 2019. Anuario estadístico de la producción agrícola (aguacate). Servicio de Información Agroalimentaria y Pesquera http://infosiap.siap.gob.mx/aagricola_siap_gb/icultivo/index.jsp (last accessed 2 Oct 2019).

Tapia Rodríguez A, Ramírez Dávila JF, Salgado Siclán ML, Castañeda Vildózola Á, Maldonado Zamora FI, Lara Díaz AV. 2020. Distribución espacial de antracnosis (*Colletotrichum gloeosporioides* Penz) en aguacate en el Estado de México, México. Revista Argentina de Microbiología 52: 72–81.

Thomas CFG, Parkinson L, Griffiths GJK, Fernandez Garcia A, Marshall EJP. 2001. Aggregation and temporal stability of carabid beetle distributions in field and hedgerow habitats. Journal of Applied Ecology 38: 100–116.

Zhang X, Zhou J, Li G, Chen C, Li M, Luo J. 2020. Spatial pattern reconstruction of regional habitat quality based on the simulation of land use changes from 1975 to 2010. Journal of Geographical Sciences 30: 601–620.